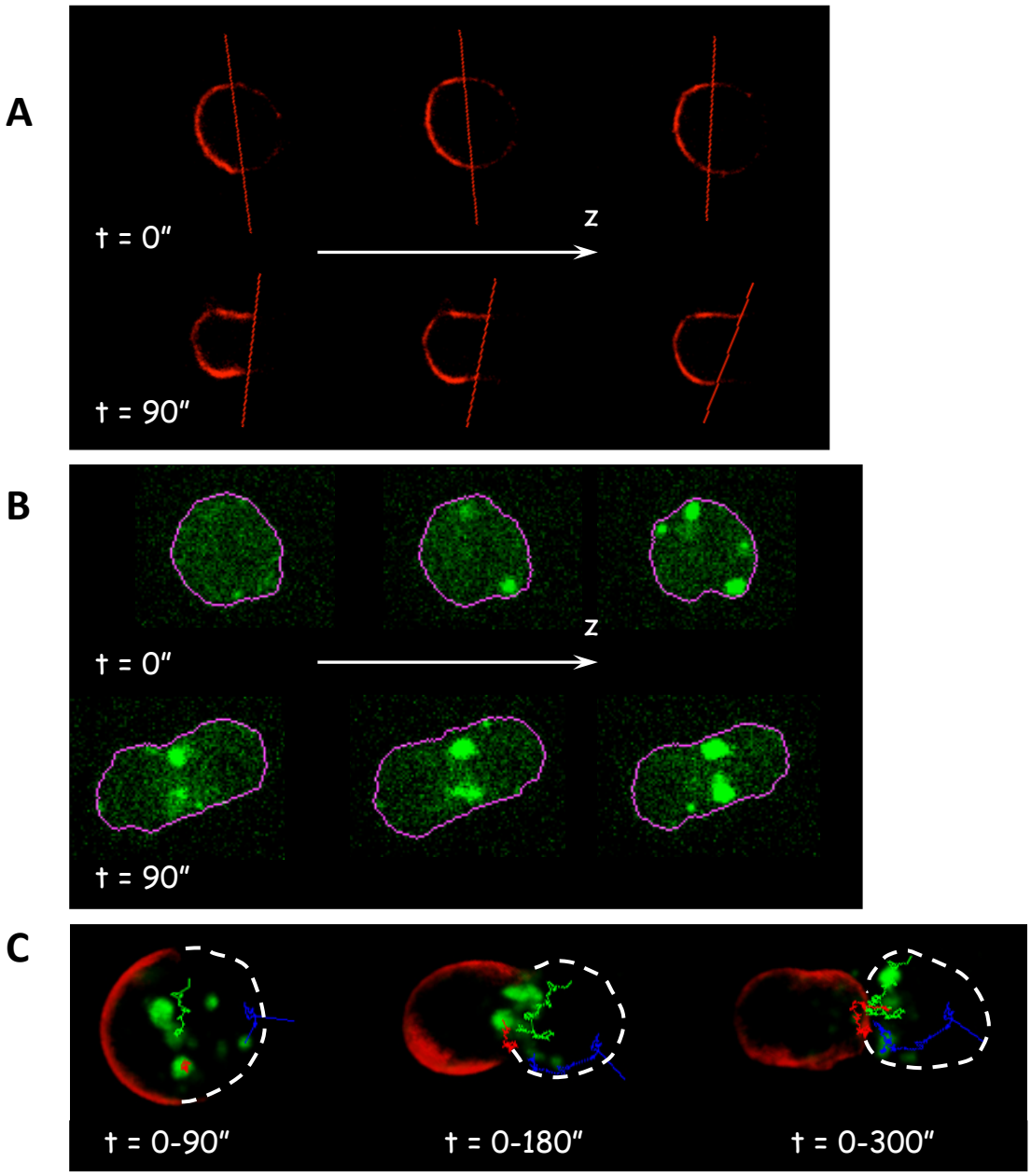

Figure 1. Automated 4D detection and tracking of endosomes and polarity markers.

A: Three different z planes of a dividing SOP shown at two different time-points illustrate the automated detection of the Pon crescent limit (straight red line).

B: Three different z planes of a dividing SOP shown at two different time-points illustrate the automated detection of the cell outline (purple line).

C: Illustration of the tracks of three endosomes (red, green and blue lines) during the division of an SOP. In green is Sara-GFP, in red is Pon-RFP. The white dashed line delimitates the part of the SOP that will form the pIIa cell (C).

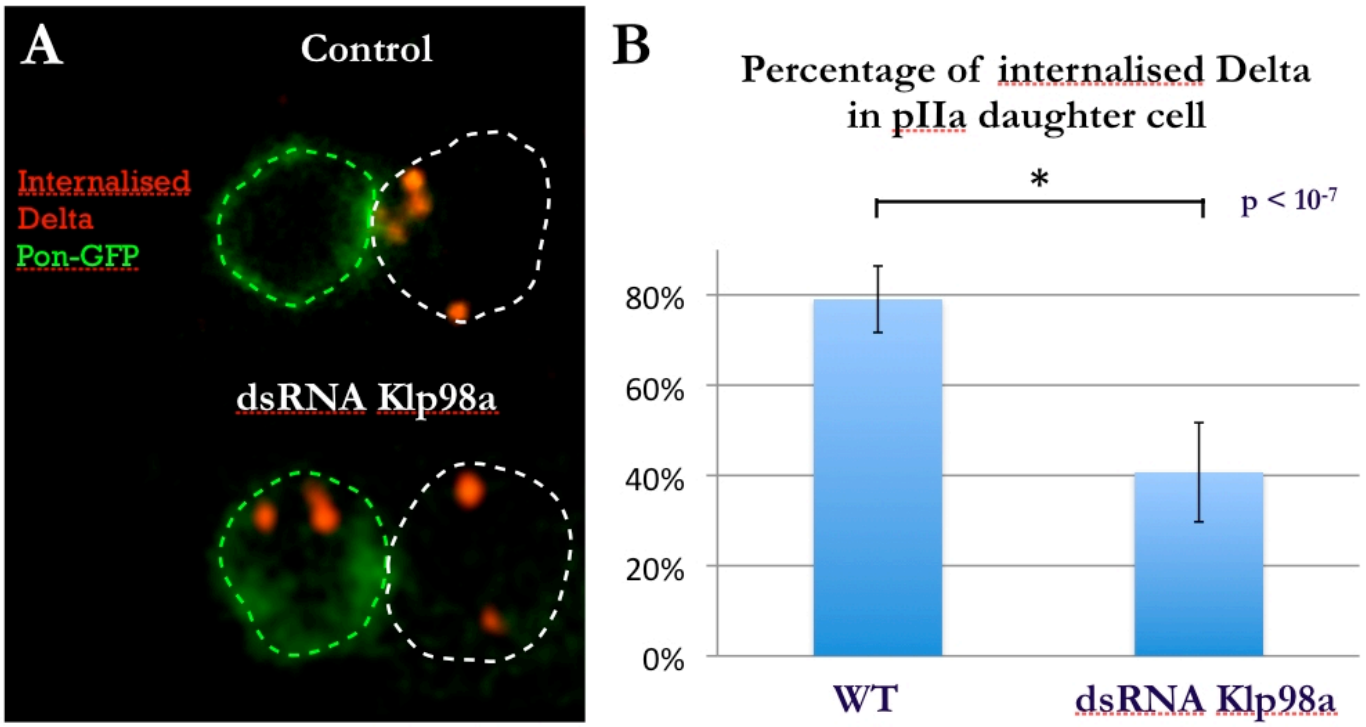

Figure 2. Down-regulation of Klp98a induces a symmetrical partitioning of Sara endosomes.

A, B: Sara endosomes partitioning in a control SOP (A) and upon RNAi of Klp98a (B). Sara endosomes are marked by internalised Delta (in red), Pon-GFP (in green) marks the pIIb daughter cell and the pIIa and pIIb outlines are represented by the white and green dashed lines respectively.

C: The ratio of internalised Delta segregating to the pIIa versus the pIIb daughter cell has been normalised with the mean volume of the cells and measured in control SOPs (n=22 cells) and upon down-regulation of Klp98a (n=21 cells).

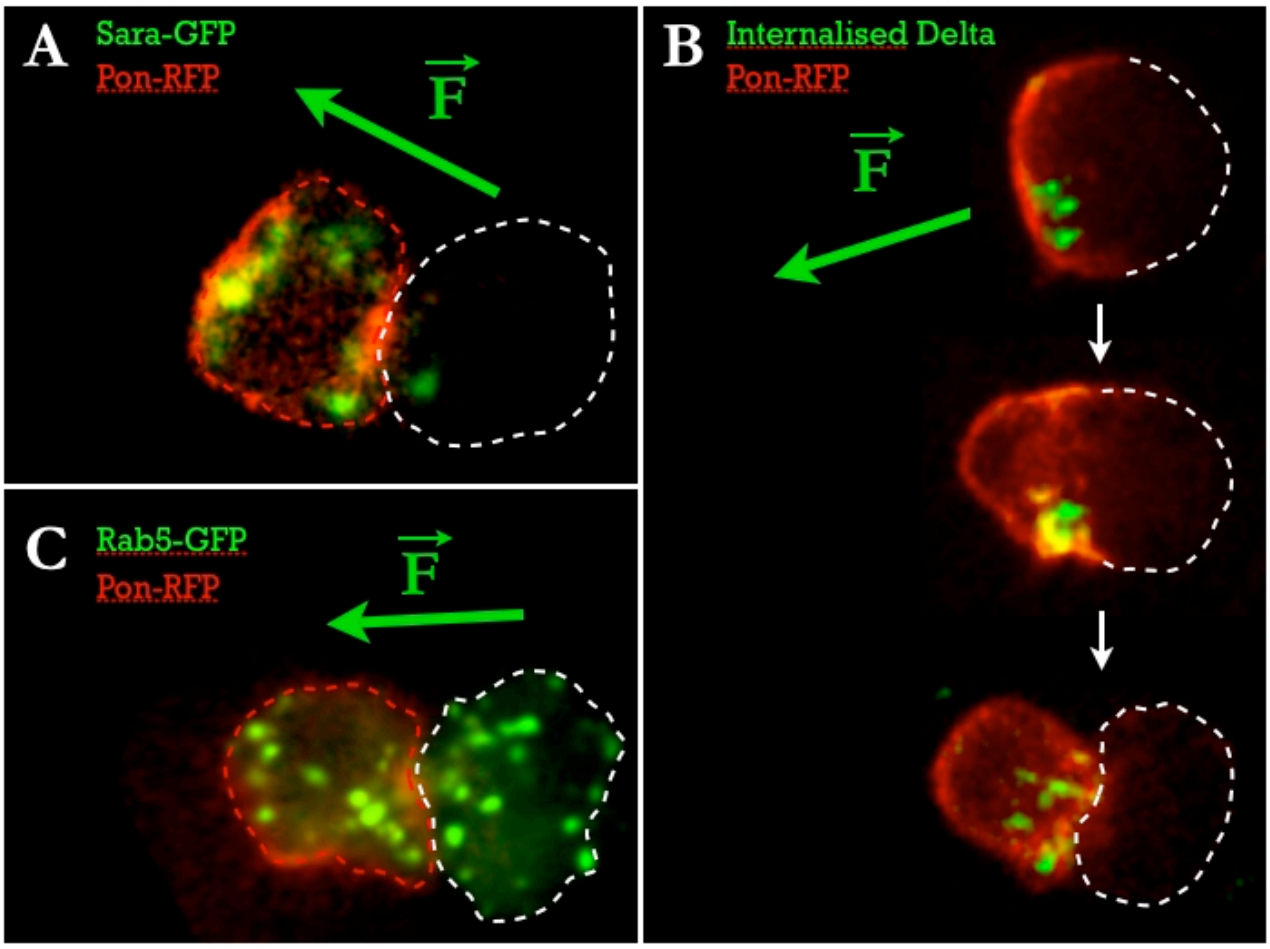

Figure 3. Specific magnetic micro-manipulation of Sara endosomes.

SOP cells have internalised magnetic nanoparticles in a pulse-chase protocol to target them to Sara endosomes, and have been submitted to a magnetic force while their division was being imaged with a spinning-disc microscope.

A: Sara endosomes marked by Sara-GFP can be mis-segregated to the pIIb daughter cell (compare with fig. 6A).

B: Three stills from a time-lapse movie in which Sara endosomes marked by internalised Delta were mis-segregated to the pIIb daughter cell (compare with fig. 2A).

C: The bulk of early endosomes (marked by Rab5-GFP) is still symmetrically partitioned in these conditions.

In all panels the green arrow represents the direction of the magnetic force applied. Pon-RFP marks the pIIb daughter cell, and the pIIa and pIIb outlines are represented by white and red dashed lines, respectively.

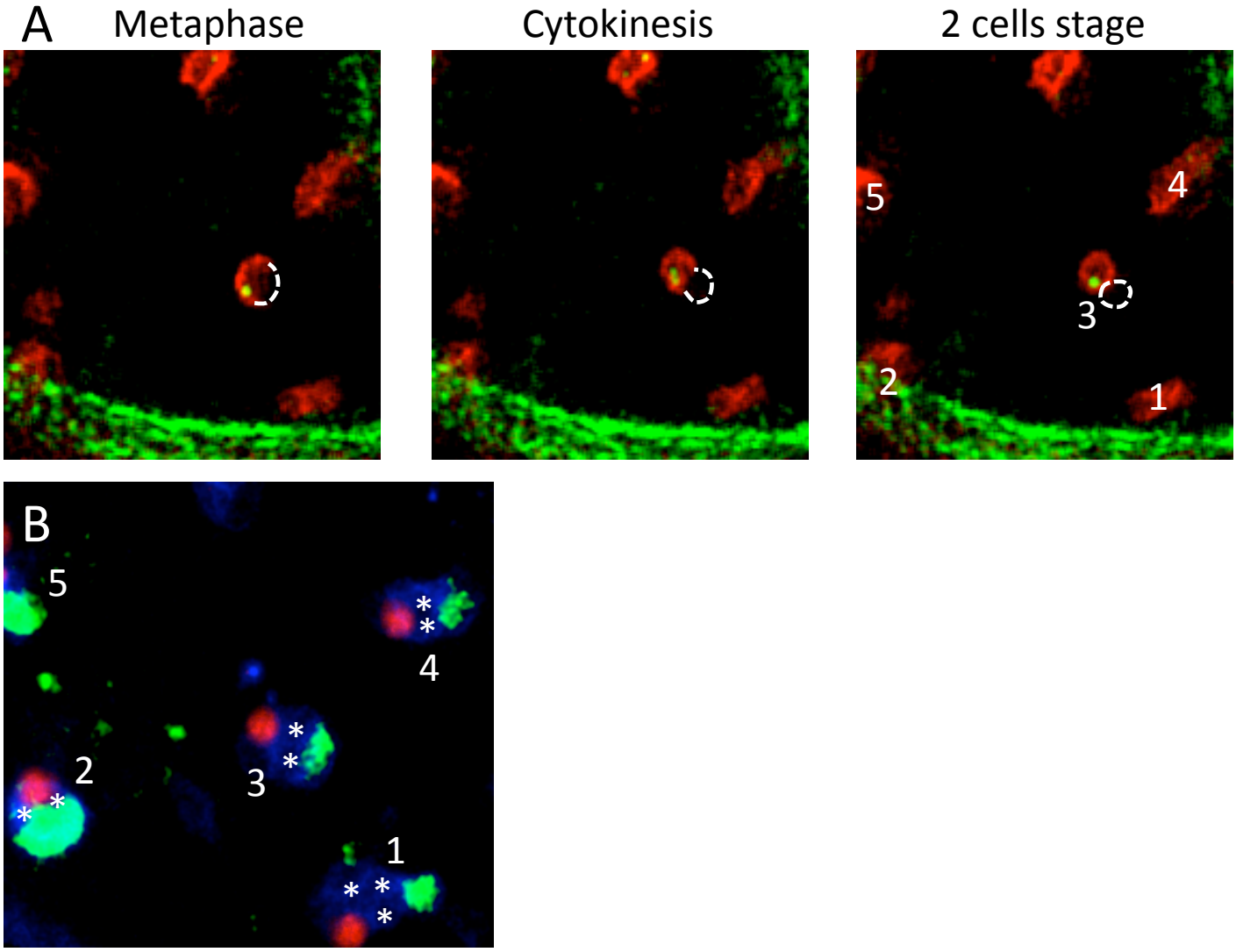

Figure 4. Sara endosomes mis-segregation is not sufficient to induce cell fate changes, as revealed by correlative live imaging and lineage analysis.

A: The notum of a Drosophila expressing Pon-RFP under the control of an SOP-specific promoter has been dissected and imaged with a confocal microscope. Pon-RFP (in red) marks the cortex of interphase SOPs, the anterior cortex of dividing SOPs (A1 and A2) and the cortex of pIIb daughter cells (A3). The dotted white line marks the posterior cortex of dividing SOPs (A1 and A2) and the cortex of pIIa daughter cells (A3).

B: The notum explant has been cultivated during 12 hours, fixed and processed for immunofluorescence. Su(H) (green) marks socket cells and Elav (red) marks neurons; Pon-RFP (blue) marks sensory organ cells and the asterisks mark shaft, sheath and glial cells of sensory organs.

In A and B the numbers (1-5) mark sensory organ precursor cells (in A) and their respective progeny (in B).

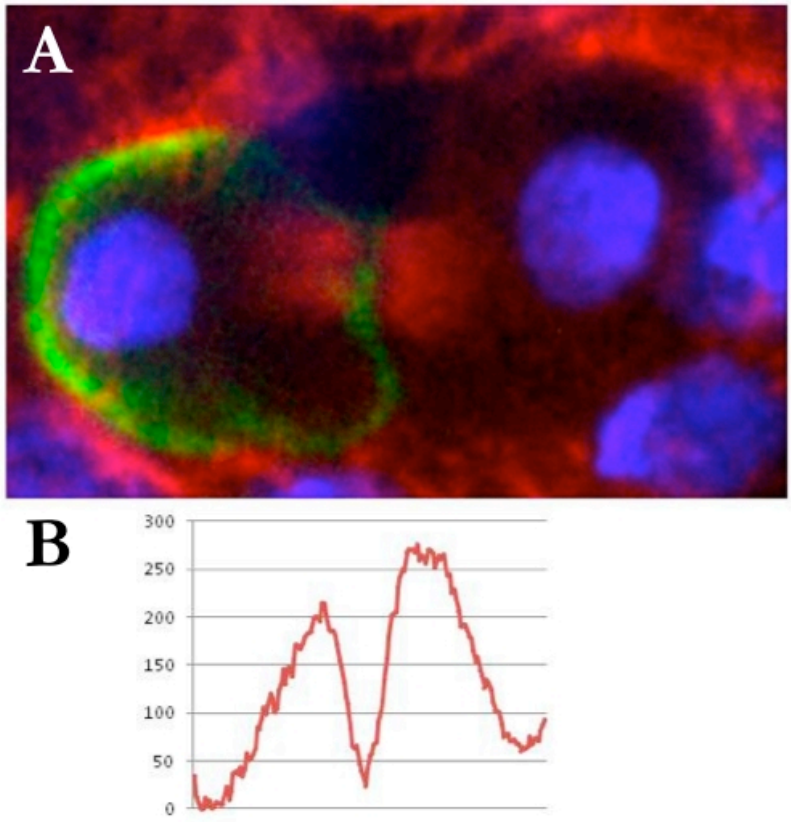

Figure 5. Asymmetric quantities of acetylated tubulin on the central spindle.

A: Staining of acetylated tubulin in an SOP cell in cytokinesis. The anterior pIIb cell (on the left) is marked by Pon-GFP, in green; the posterior pIIa cell is on the right. In blue is DAPI.

B: Plot profile of acetylated tubulin intensity measured on the spindle along the antero-posterior axis.

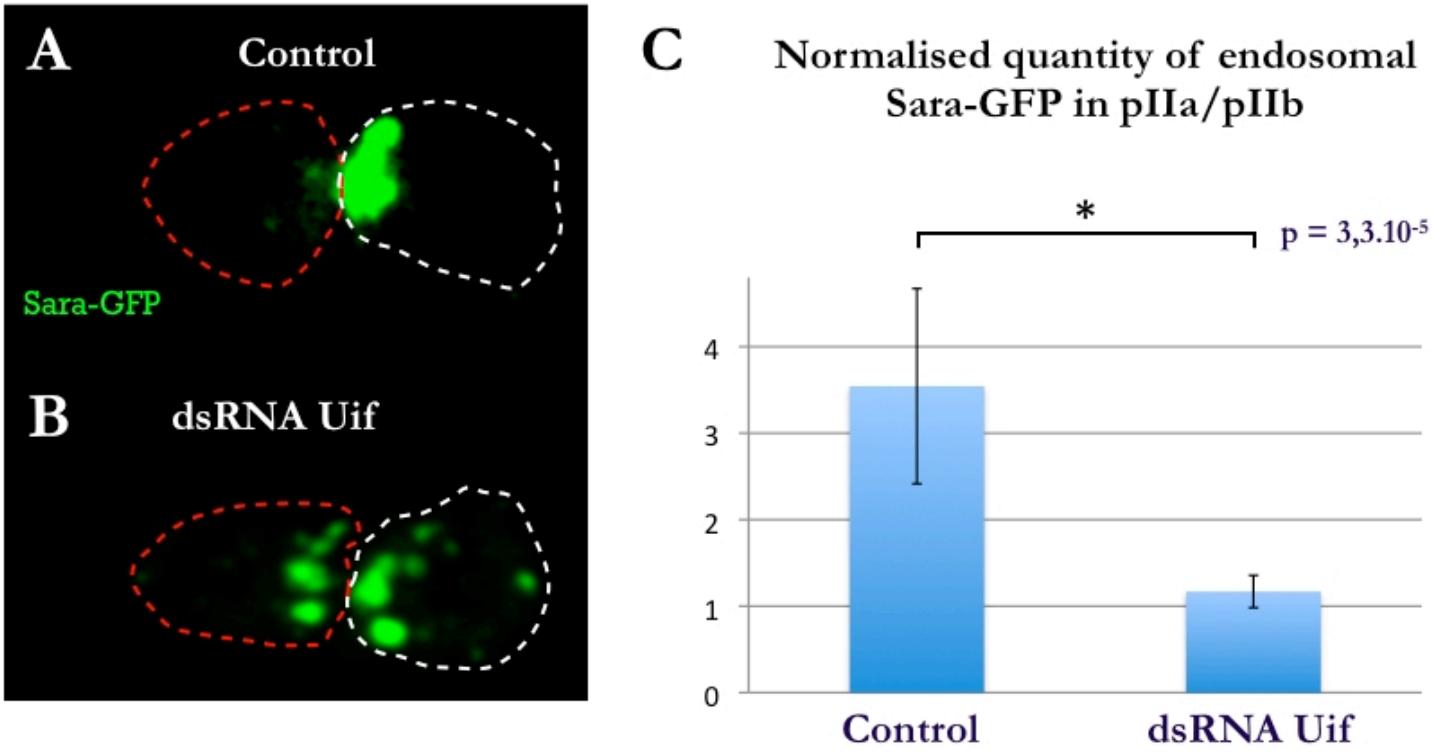

Figure 6. Down-regulation of Uif induces a symmetrical partitioning of Sara endosomes.

A, B: Sara endosomes partitioning in a control SOP (A) and upon RNAi of Uif (B). Sara endosomes are marked by Sara-GFP and the pIIa and pIIb outlines are represented by the white and red dashed lines respectively.

C: The ratio of endosomal Sara-GFP segregating to the pIIa versus the pIIb daughter cell has been normalised with the mean volume of the cells and measured in control SOPs (n=24 cells) and upon down-regulation of Uif (n=15 cells).

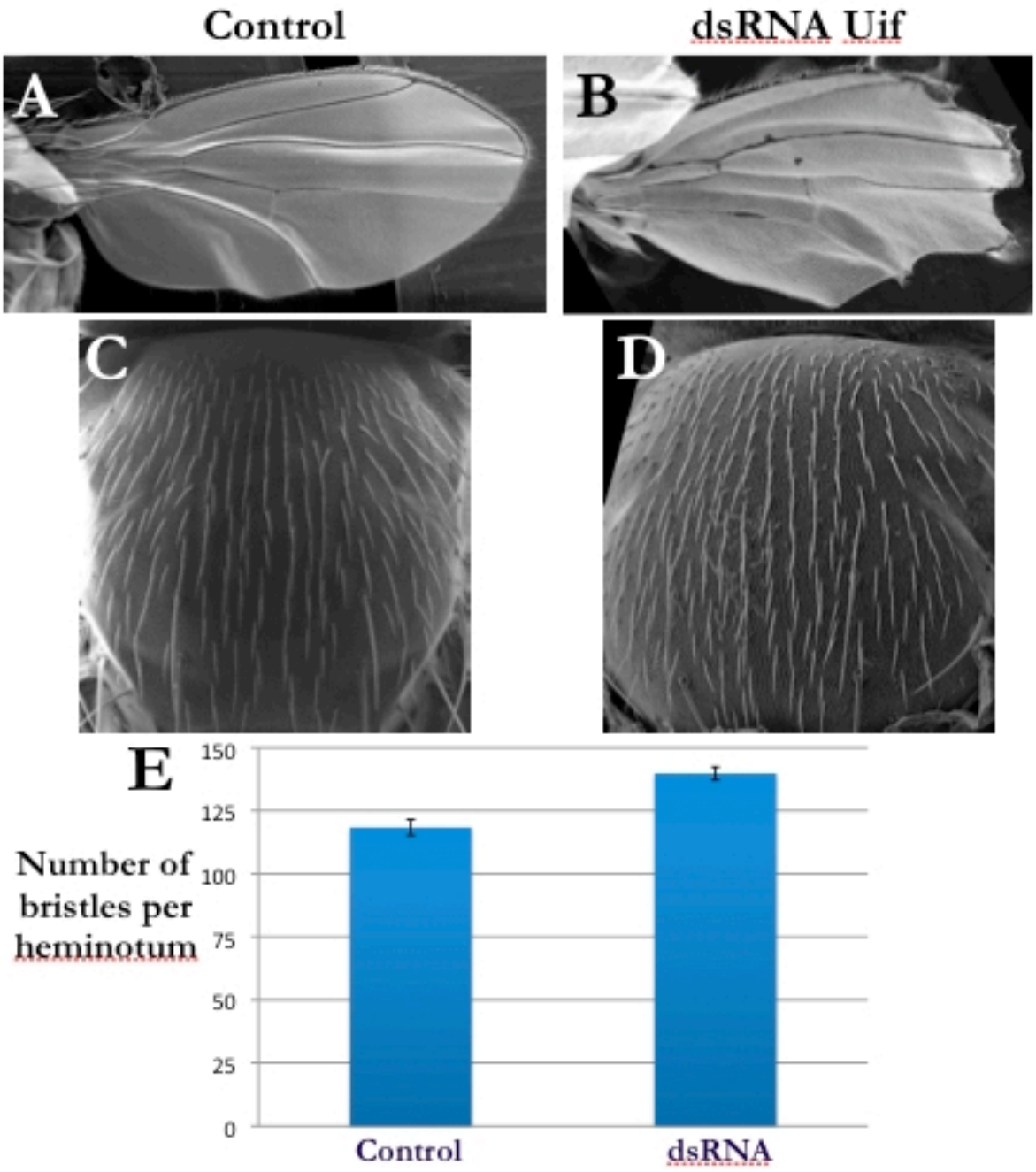

Figure 7. Down-regulation of Uif induces Notch loss-of-function phenotypes in the wing and on the notum.

A-D: Scanning electron microscopy pictures of wings (A,B) and nota (C,D) of control flies (A,C) and flies expressing a dsRNA against Uif (B,D).
E: Quantification of the number of sensory organs observed on heminota of control flies and upon down-regulation of Uif.
The notched wings and the increased number of sensory organs are both reflective of a Notch loss-of-function phenotype.